



The University of Bradford Institutional Repository

<http://bradscholars.brad.ac.uk>

This work is made available online in accordance with publisher policies. Please refer to the repository record for this item and our Policy Document available from the repository home page for further information.

To see the final version of this work please visit the publisher's website. Available access to the published online version may require a subscription.

Link to publisher's version: <https://doi.org/10.3906/elk-1510-100>

Citation: Zhang Y, Lazardis P, Abd-Alhameed RA and Glover I (2016) A compact wideband printed antenna for free-space radiometric detection of partial discharge. Turkish Journal of Electrical Engineering & Computer Sciences. 25: 1291–1299.

Copyright statement: © 2016 TÜBİTAK. Reproduced in accordance with the publisher's self-archiving policy.

1 **A compact wideband printed antenna for free-space radiometric**
2 **detection of partial discharge**

3 Yong ZHANG^{1,*}, Pavlos LAZARIDIS¹, Raed ABD-ALHAMEED², Ian GLOVER¹

4 ¹Department of Engineering & Technology, University of Huddersfield, Huddersfield, UK

5 ²School of Electrical Engineering & Computer Science, University of Bradford, Bradford, UK

6 *Correspondence: y.zhang@hud.ac.uk

7 **Abstract:** A microstrip line-fed wideband printed antenna is presented for radio
8 detection of partial discharge (PD). The novel simple structure antenna has compact size
9 of $24 \times 20 \times 0.16 \text{ cm}^3$ ($0.28\lambda_s \times 0.23 \lambda_s \times 0.002 \lambda_s$) and suitable for radiometric PD
10 wireless sensor nodes, where λ_s is the wavelength of the lowest frequency of the band
11 (i.e., 0.35 GHz). The stepped and beveled radiation patch is used in combination with a
12 slotted ground plane to achieve a wide fractional bandwidth of 119% (0.35 to 1.38
13 GHz) for a return loss better than 10 dB. Good radiation pattern characteristics are
14 obtained across the frequency band of interest. The match between simulated and
15 experimental results suggests that the design is sound and robust.

16 **Key words:** Wideband, compact size, printed antenna, partial discharge, radio
17 detection.

18 **1. Introduction**

19 **Partial discharge (PD)** may occur when a usually-earthed metallic component in an item
20 of **high voltage (HV)** plant becomes disconnected from ground. PD monitoring can play
21 a valuable role in the on-going maintenance of HV plant. The location of PD sources by
22 free-space radio detection is an attractive approach for condition monitoring of HV
23 equipment in electricity substations. A suggested band for radio PD detection is 0.3–1.5
24 GHz [1]. A low-cost, radiometric, PD wireless sensor network (WSN) has been

1 proposed to provide real-time coverage for an entire substation [2]. The PD WSN is a
2 collection of broadband radiometer sensors that measure PD activity interfaced to
3 WirelessHART modules. The WirelessHART modules relay the PD activity data to an
4 access point via wireless links. The access point is interfaced to a network and security
5 manager and may also be interfaced to network gateway. For such PD detection
6 systems, the design of radiometer antennas is one of the major challenges.

7 Several antennas for PD detection have recently been reported [1, 3–5]. These antennas,
8 however, address multi-narrow-band operation [1, 4] or achieve only modest VSWR
9 performance ($VSWR < 5$) [3] or only work at higher frequency band (0.75–1.5 GHz)
10 and have no detailed specification [5]. Wideband antennas, operating in the lower radio
11 frequency (RF) band include discone antennas, biconical antennas, log-periodic
12 antennas and spiral antennas. These antennas are larger, heavier and more expensive
13 than is practical for a dense PD wireless sensor network comprising many tens or even
14 hundreds of radiometer sensor nodes. The design of radiometer antennas must meet
15 some key requirements such as being light in weight, compact in size, low in
16 manufacturing cost and allowing easy integration with a compact RF receiver. A novel
17 simple structure broadband printed antenna meeting these requirements is presented
18 here for PD detection applications. The compact antenna has satisfactory performance
19 over the frequency band 0.35 GHz to 1.38 GHz with small size of around $\lambda_s/4$ (where λ_s
20 is the wavelength of the lowest frequency of the band, i.e., 0.35GHz).

21 **2. Radiated PD**

22 PD comprises short-duration current pulses that occur predominantly in the first and
23 third quadrants of the power system cycle. The frequency spectrum of the pulses has
24 measurable energy extending well into the gigahertz region and a significant fraction of

1 this energy is radiated from the conductors close to the PD source. Figure 1a shows a
2 typical PD current pulse. The PD current pulse has short duration of the order of
3 nanoseconds with a measurable energy spectrum extending up to several gigahertz. It
4 is often approximated by a Gaussian waveform with half-amplitude width $T_l + T_h$ [4],
5 given by

$$6 \quad I(t) = I_0 e^{-(t/t_0)^2} \quad (1)$$

7 where $t_0 = (T_l + T_h) / 2\sqrt{\log 2}$. The rise time T_l is usually less than the fall time T_h .

8 PD activity occurring inside a closed metallic chamber, e.g. the interior of an item of
9 gas insulated switchgear (GIS) or a transformer tank, results in a radiated signal that has
10 been subject to multiple reflections. Electromagnetic signal radiated by PD current
11 pulses have a time waveform and a frequency spectrum that depends on the impulse
12 response of the radiating structure. Figure 1b shows a measured radiated signal. A cost-
13 effective radiometric detection system is designed to measure PD radiated signal.
14 Compact broadband antenna is a key component of such detection system. **The designed**
15 **antenna has successfully been applied to radiometric WSN for PD detection and**
16 **location, shown in Figure 2, with good performance.**

17 **3. Antenna Design**

18 The antenna has been constructed on FR4 substrate with thickness 1.6 mm and
19 dielectric constant 4.9. The dimensions and constructed prototype are shown in Figure
20 3. It comprises a rectangular patch on one side of the substrate and a ground plane on
21 the other side. The patch is fed by a 50 Ω microstrip transmission line of width 3 mm
22 (W_2).

23 In most cases, the well matched antenna is simply represented by a 50 Ω resistive load.

24 For broadband antennas, the matching bandwidth can be achieved by overlapping

1 several adjacent resonances, each which can be represented by an RLC parallel circuit
2 [6], Figure 4. A smooth transition between adjacent resonances ensures good impedance
3 match over a broad frequency range.

4 The monopole antenna and ground plane form an equivalent dipole antenna [7]. The
5 simple structure antenna is compact (dimensions 200 mm (W) × 240 mm (L)). The
6 overall size of the antenna configuration is around $\lambda_s/4$ instead of $\lambda_s/2$ for the lower edge
7 of the operating frequency. The low frequency limit is determined by the total effective
8 length of the antenna current distribution, which includes the radiation patch and ground
9 plane [8]. The frequency corresponding to the lower resonance of a rectangular planar
10 monopole can be approximately given by

$$11 \quad f_r = \frac{144}{L + r_1 + r_2} \text{ GHz} \quad (2)$$

12 and

$$r_1 = \frac{A_g}{2\pi\sqrt{\epsilon_{re}}L_1} \quad (3)$$

$$13 \quad r_2 = \frac{A_p}{2\pi\sqrt{\epsilon_{re}}(L - L_1 - L_3)} \quad (4)$$

14 where A_g and A_p are the area of the ground plane and the radiation patch respectively.

15 $\epsilon_{re} = (1 + \epsilon_r)/2$ is the effective dielectric constant of the composite dielectric. All
16 dimensions are in millimeters. When the desirable frequency band of antenna is
17 available, the antenna size can be compact by optimizing the area and structure of
18 ground and radiation patch.

19 Slots of dimensions ($W_3 \times L_4$) are cut into the patch shoulders to electromagnetically
20 couple the patch and ground plane. This significantly increases impedance bandwidth.

21 The patch shoulders and bevels result in gradual variation of the distance from the patch
22 to the ground plane. As a consequence, the impedance change from one resonance to

1 another is small ensuring good impedance match over a broad frequency range. Figure 5
2 shows the simulated return loss curves for different slot sizes L_4 when other parameters
3 are kept unchanged. The gap L_3 between patch and ground plane introduces a coupling
4 capacitance that further improves impedance matching over the broadband band [7–9].
5 The simulated return loss curves with different values of L_3 are plotted in Figure 6. The
6 electromagnetic coupling between the lower edge of the patch and the ground plane can
7 be properly controlled by adjusting L_3 . The optimized gap distance is chosen as 2 mm.
8 The leaky current between radiating patch and ground plane results in capacitive
9 coupling. Larger gap L_3 leads to weaker coupling therefore worse impedance matching.
10 The ground plane is an integral part of the radiating configuration and its current
11 distribution significantly affects the overall antenna characteristics. The rectangular
12 notch in the ground plane improves both impedance matching and radiation
13 characteristics at high frequency. Figure 7 and 8 show the simulated return loss for
14 various values of W_1 and L_2 when L_3 is fixed at 2 mm. The simulated return loss curves
15 with different values of W_3 are plotted in Figure 9, which shows that W_3 has a modest
16 effect on antenna performance. Detailed investigation and extensive simulations have
17 been undertaken with CST Microwave Studio to optimise the antenna structure and
18 parameters: $L_1 = 40$ mm, $L_2 = 6$ mm, $L_3 = 2$ mm, $L_4 = 43$ mm, $L_5 = 100$ mm, $W_1 = 64$
19 mm, $W_2 = 3$ mm, $W_3 = 16$ mm, $W_4 = 50$ mm, $W_5 = 68$ mm, $h = 1.6$ mm.

20 **4. Results and Discussions**

21 The measurements were made in an anechoic chamber using a vector network analyzer.
22 Figure 10 shows the measured and simulated return loss. The return loss (S11) -10 dB
23 fractional bandwidth is 119% (from 0.35 to 1.38 GHz). The second resonance occurs at
24 0.77 GHz in the simulation but is not apparent in the measurement. This could be due to

1 the effect of the SMA port. The normalized yz -plane (E-plane) and xz -plane (H-plane)
2 radiation patterns have been simulated and measured at 0.45, 0.7 and 1 GHz, Figure 11–
3 13. The xz -plane patterns are approximately omnidirectional over the operating
4 frequency range. The yz -plane patterns have generally good symmetry. The symmetry
5 becomes less good at the highest measurement frequency as the dimensions of the
6 antenna become comparable to wave length. Overall, the radiation patterns of the
7 antenna are very similar to those of a conventional monopole antenna. The simulated
8 3D radiation pattern is shown at 0.55GHz as an example in Figure 14.

9 The calculated variation of maximum gain with frequency is shown in Figure 15. The
10 gain is 1.7 to 5.1 dBi over the design band. The figure indicates that the proposed
11 antenna has good gain flatness with gain variation of less than 3.5 dBi throughout the
12 entire frequency band. The gain decreases at lower frequency band due to compact
13 antenna size. Antenna gain is proportional to the effective radiation aperture. The
14 antenna efficiency of the proposed antenna is equal to the radiation efficiency minus the
15 return loss. The antenna efficiency has a maximum value of 93% and a minimum value
16 of 54% within the frequency range from 0.35–1.38 GHz. The average antenna
17 efficiency is 81%. It is possible that information about the type and severity of
18 insulation defect resides in the time series of received partial discharge pulses. If such
19 information is to be extracted from the received signals then shape of the pulses must be
20 retained. This implies a linear phase (constant group delay) antenna since such an
21 antenna (assuming constant gain across its passband) will not significantly distort the
22 received signal. In this case pulse dispersion must be minimised and group delay will be
23 important. Figure 15 presents the simulated group delay which varies by less than 2 ns
24 from its mean value over most of the operating frequency band. This means that the

1 broadband antennas have good transient response in the working band. The table below
2 shows the comparison between the proposed antenna and other reported antennas for
3 PD detection.

4 **5. Conclusion**

5 A compact microstrip-fed planar broadband antenna for PD detection applications has
6 been presented. The antenna satisfies a -10 dB return loss requirement from 0.35 to 1.38
7 GHz. The radiation pattern is close to that of a simple monopole. Predicted variation in
8 group delay is not more than 2 ns. The proposed broadband antenna provides wider
9 impedance bandwidth than the single or multiple narrowband antenna in [1, 4] and the
10 Hilbert antenna ($VSWR < 5$) in [3] to collect more PD energy for higher radiometric
11 sensitivity. The antenna is compact, light and inexpensive to manufacture making it
12 suitable for use in a dense sensor network.

13 **Acknowledgements**

14 This work was supported by the U.K. Engineering & Physical Sciences Research
15 Council (EPSRC) under grant EP/J015873.

16 **References**

- 17 [1] Ye H, Qian Y, Dong Y, Sheng G, Jiang X. Development of multi-band ultra-high-
18 frequency sensor for partial discharge monitoring based on the meandering technique.
19 IET Sci Meas Technol 2014; 8: 327–335.
- 20 [2] Zhang Y, Upton D, Jaber A, Ahmed H, Saeed B, Mather P, Lazaridis P, Mopty A,
21 Tachtatzis C, Atkinson R, et al. Radiometric wireless sensor network monitoring of
22 partial discharge sources in electrical substations. Int J Distrib Sens N 2015; 438302: 1–
23 9.

1 [3] Li J, Wang P, Jiang T, Bao L, He Z. UHF stacked Hilbert antenna array for partial
2 discharge detection. *IEEE Trans Antennas Propag* 2013; 61: 5798–5801.

3 [4] Shibuya Y, Matsumoto S, Konno T. Electromagnetic waves from partial discharges
4 in windings and their detection by patch antenna. *IEEE Trans Dielectr Electr Insul*
5 2011; 18: 2013–2023.

6 [5] Lopez-Roldan J, Tang T, Gaskin M. Optimisation of a sensor for onsite detection of
7 partial discharges in power transformers by the UHF method. *IEEE Trans Dielectr*
8 *Electr Insul* 2008; 15: 1634–1639.

9 [6] Pele I, Chousseaud A, Toutain S. Simultaneous modeling of impedance and
10 radiation pattern antenna for UWB pulse modulation. In: *IEEE 2004 Antennas and*
11 *Propagation Society International Symposium*; 20–25 June 2004; Monterey, California,
12 USA: IEEE. pp. 1871–1874.

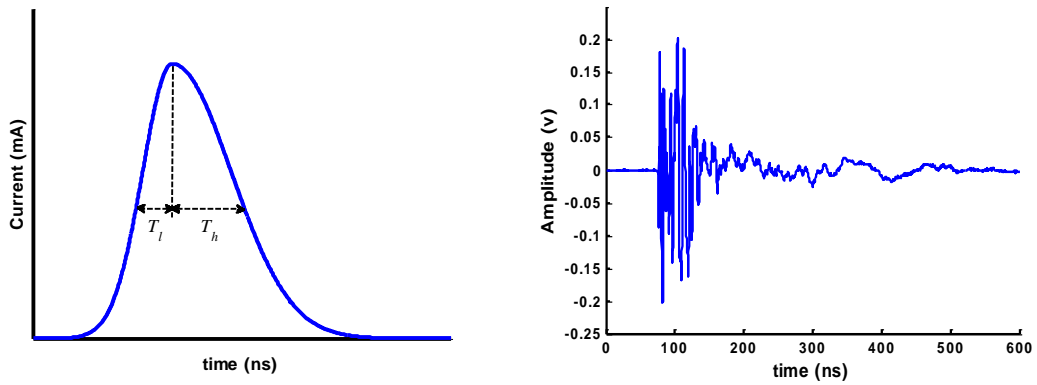
13 [7] Jiang W, Che W. A novel UWB antenna with dual notched bands for WiMAX and
14 WLAN applications. *IEEE Antennas Wireless Propag Lett* 2012; 11: 293–296.

15 [8] George Thomas K., Sreenivasan M. A simple ultrawideband planar rectangular
16 printed antenna with band dispensation. *IEEE Trans Antennas Propag* 2010; 58: 27–34.

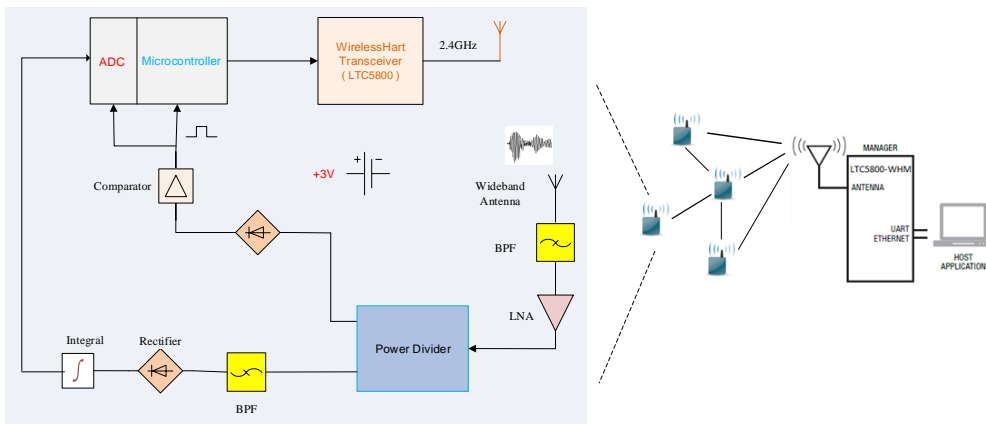
17 [9] Hong C, Ling C, Tarn I, Chung S. Design of a planar ultrawideband antenna with a
18 new band-notch structure. *IEEE Trans Antennas Propag* 2007, 55: 3391–3397.

19

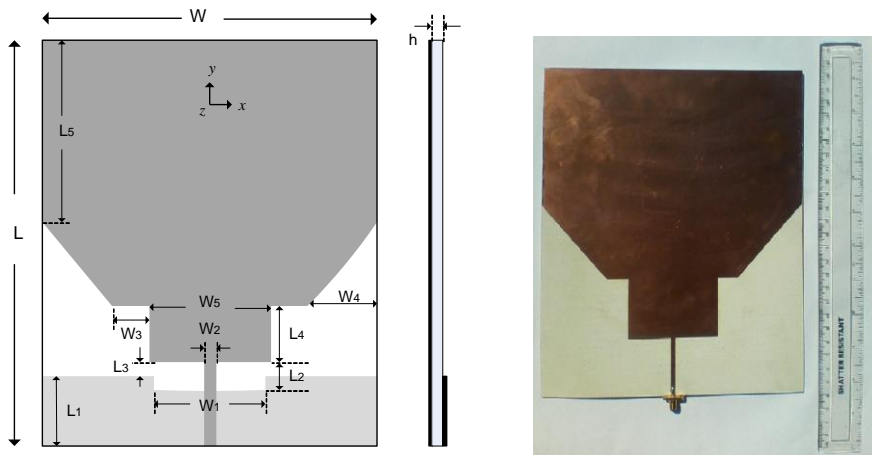
20



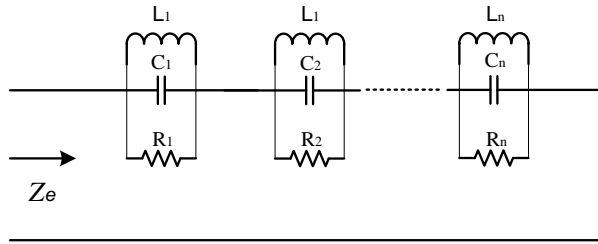
1
 2 **Figure 1.** (a) Typical PD current pulse, (b) Typical signal arising from radiated PD
 3 energy.



4
 5 **Figure 2.** Radiometric wireless sensor network for PD detection and location.



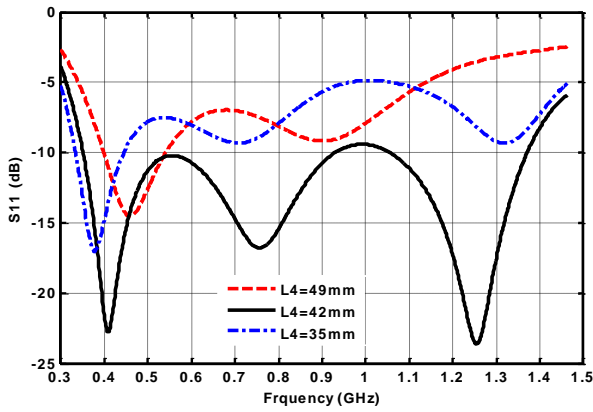
6
 7 **Figure 3.** Antenna configuration and constructed prototype



1

2

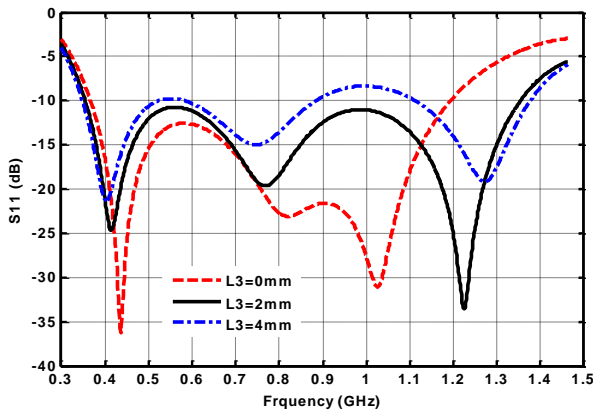
Figure 4. Equivalent circuit model of UWB antenna



3

4

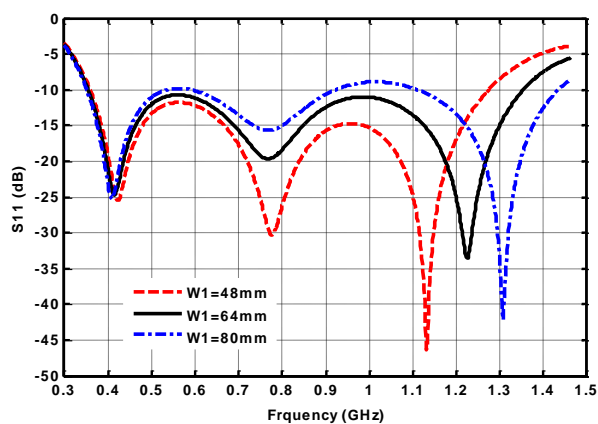
Figure 5. Simulated return loss for different L_4 .



5

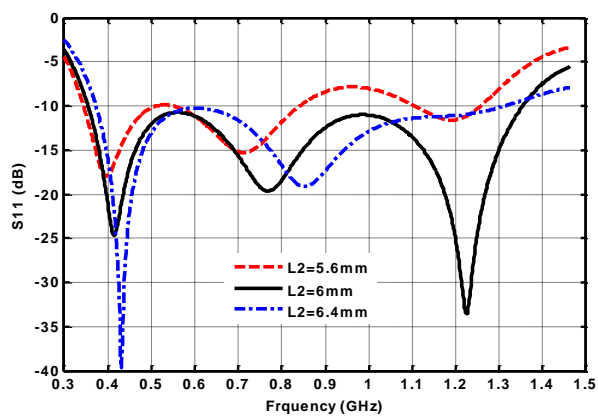
6

Figure 6. Simulated return loss for different L_3



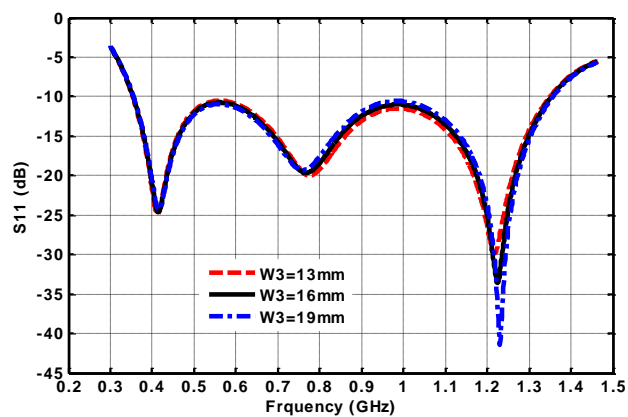
1

2 **Figure 7.** Simulated return loss for different W_1 .



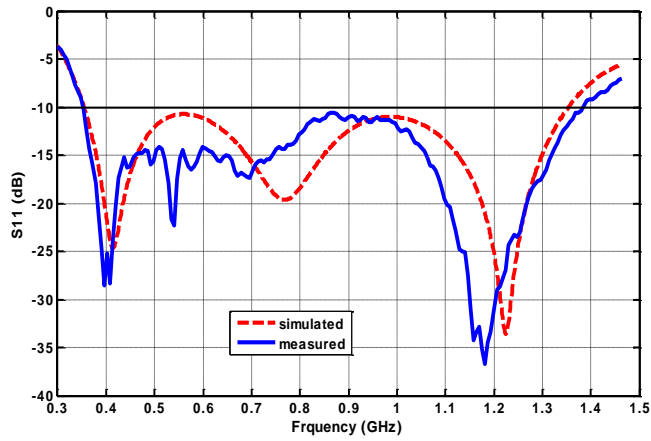
3

4 **Figure 8.** Simulated return loss for different L_2 .

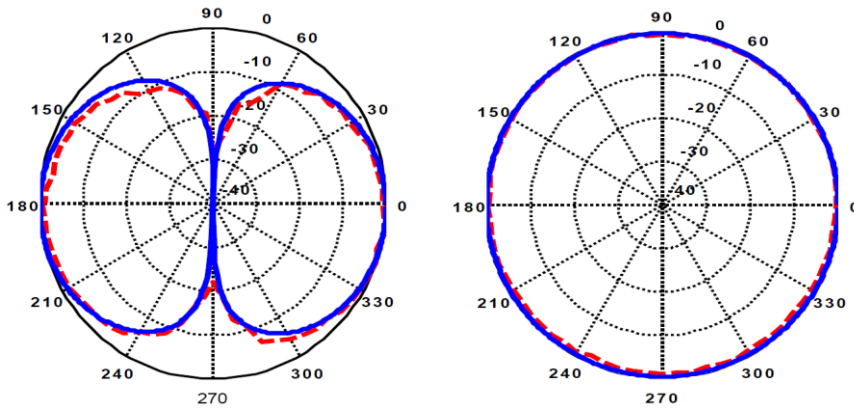


5

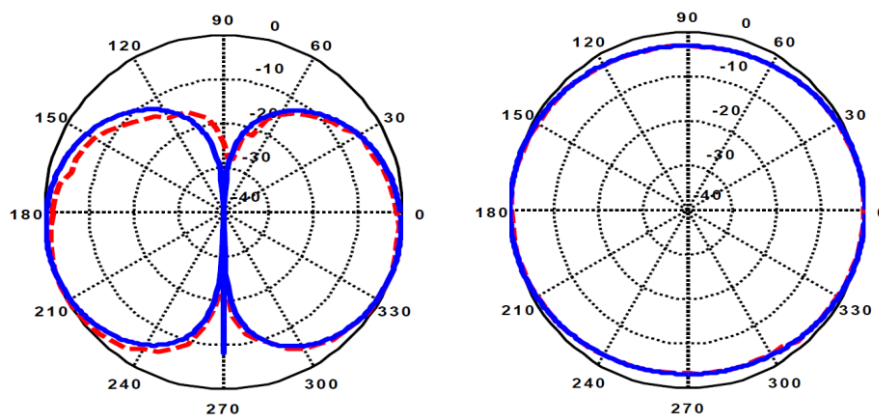
6 **Figure 9.** Simulated return loss for different W_3 .



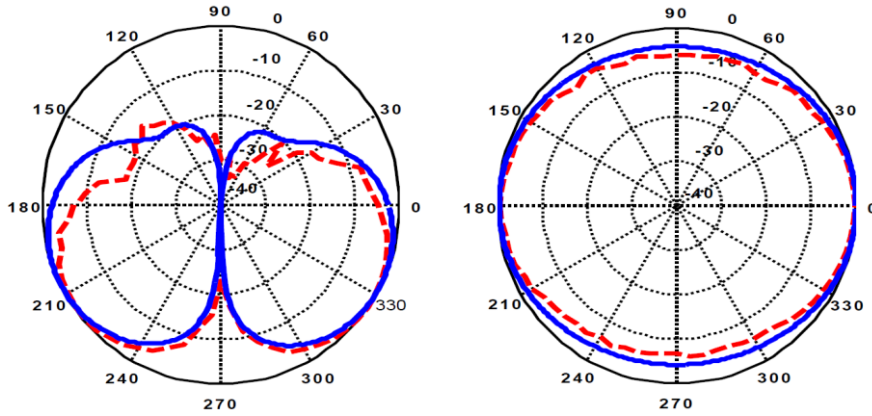
1
2 **Figure 10.** Simulated and measured return loss



3
4 **Figure 11.** Simulated and measured radiation patterns in the yz and xz plane at 0.45
5 GHz. (Solid lines: denote simulations, dashed lines: denote measurements.)



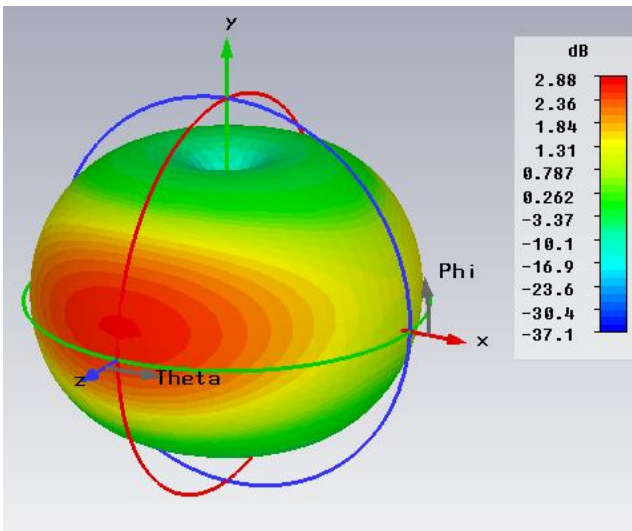
6
7 **Figure 12.** Simulated and measured radiation patterns in the yz and xz plane at 0.7
8 GHz. (Solid lines: denote simulations, dashed lines: denote measurements.)



1

2 **Figure 13.** Simulated and measured radiation patterns in the yz and xz plane at 1 GHz.

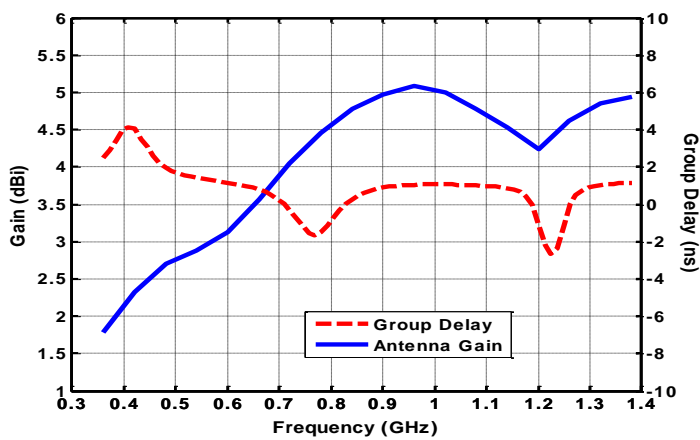
3 (Solid lines: denote simulations, dashed lines: denote measurements.)



4

5

6 **Figure 14.** Simulated 3D radiation pattern at 0.55 GHz.



7

8 **Figure 15.** Antenna gain and group delay

1 **Table.** Performance comparison of various antennas

Antennas \ parameters	Bandwidth (MHz)	VSWR	Dimension (cm)
The proposed antenna	350 – 1380	< 2	24 × 20
Antenna in Reference 1	480 – 520 800 – 850 1100 – 1200	< 2	19.12 (diameter)
Antenna in Reference 3	339 – 375 395 – 440 450 – 1000	< 5	7 × 7
Antenna in Reference 4	1800 narrowband	< 2	4.19 × 2.94

2